Comparative Evaluation of 4-Dimensional Computed Tomography and 4-Dimensional Magnetic Resonance Imaging to Delineate the Target of Primary Liver Cancer

Yukai Chen[1] [ORCID]**, Guanzhong Gong[2], Yinxing Wang[2], Chenlu Liu[3], Ya Su[2], Lizhen Wang[2], Bo Yang[1], and Yong Yin[2]**

Abstract

Purpose: To evaluate the feasibility of 4-dimensional magnetic resonance imaging (4DMRI) in establishing the target of primary liver cancer in comparison with 4-dimensional computed tomography (4DCT). **Methods and Materials:** A total of 23 patients with primary liver cancer who received radiotherapy were selected, and 4DCT and T2w-4DMRI simulations were conducted to obtain 4DCT and T2w-4DMRI simulation images. The 4DCT and T2w-4DMRI data were sorted into 10 and 8 respiratory phase bins, respectively. The liver and gross tumor volumes (GTVs) were delineated in all images using programmed clinical workflows under tumor delineation guidelines. The internal organs at risk volumes (IRVs) and internal target volumes (ITVs) were the unions of all the phase livers and GTVs, respectively. Then, the artifacts, liver volume, GTV, and motion range in 4DCT and T2w-4DMRI were compared. **Results:** The mean GTV volume based on 4DMRI was 136.42 ± 231.27 cm^3, which was 25.04 cm^3 (15.5%) less than that of 4DCT (161.46 ± 280.29 cm^3). The average volume of ITV determined by 4DMRI was 166.12 ± 270.43 cm^3, which was 22.44 cm^3 (11.9%) less than that determined by 4DCT (188.56 ± 307.57 cm^3). Liver volume and IRV in 4DMRI increased by 4.0% and 6.6%, respectively, compared with 4DCT. The difference in tumor motion by T2w-4DMRI based on the centroid was greater than that of 4DCT in the L/R, A/P, and S/I directions, and the average displacement differences were 2.6, 2.8, and 6.9 mm, respectively. The severe artifacts in 4DCT were 47.8% (11/23) greater than in 4DMRI 17.4% (4/23). **Conclusions:** Compared with 4DCT, T2-weighted and navigator-triggered 4DMRI produces fewer artifacts and larger motion differences in hepatic intrafraction tumors, which is a feasible technique for primary liver cancer treatment planning.

Keywords

4DCT, MRI, respiratory motion simulation, liver cancer, tumor delineation, radiotherapy

Abbreviations

4DMRI, 4-dimensional magnetic resonance imaging; 4DCT, 4-dimensional computed tomography; GTV, gross tumor volume; IRV, internal organ-at-risk volume; ITV, internal target volume; TCP, tumor control probability; NTCP, normal tissue complications probability.

[1] East China University of Technology, Nanchang, Jiangxi, China
[2] Shandong Cancer Hospital and Institute, Shandong First Medical University and Shandong Academy of Medical Sciences, Jinan, Shandong Province, China.
[3] School of Nuclear Science and Technology, University of South China, Hengyang, China

Corresponding Authors:

Bo Yang, State Key Laboratory of Nuclear Resources and Environment, East China University of Technology, Nanchang 330013, Jiangxi, China.
Email: Boyang@ecut.edu.cn

Yong Yin, Department of Radiotherapy, Shandong Cancer Hospital and Institute, Shandong First Medical University and Shandong Academy of Medical Sciences, Jinan 250117, Shandong Province, China.
Email: yinyongsd@126.com

Introduction

Primary liver cancer is one of the most common cancers and the 4th most frequent cause of cancer-related death globally.[1] Radiotherapy is an effective method to improve the local control rate and survival of primary liver cancer, and the safety and efficacy of radiotherapy depend on precise delineation of the target.[2-5] The motion of organs and tumors caused by human breathing affects the accuracy of delineation of the target, which is the well-documented main factor causing radiotherapy errors.[6-8] Four-dimensional computed tomography (4DCT) is the current clinical standard in tumor motion assessment because it can assess patient-specific breathing motion for determining individual safety margins in radiation therapy.[9,10]

However, the timing of 4DCT enhancement is difficult to determine with the low soft-tissue contrast of the image, which cannot clearly display the boundary between organs and tumors, which will affect the accurate delineation of the tumor target. Some studies have shown that 4DCT significantly under-predicts target motion ranges.[11-13] Furthermore, Yamamoto et al[14] stated that 90.0% of thoracic and abdominal 4DCT images are artifact-affected. Research by Sentker et al[15] showed that image artifacts in 4DCT treatment planning data negatively influence clinical outcomes in SBRT of lung and liver metastases.

MRI has higher soft-tissue resolution and higher sensitivity and specificity, enabling better clinical detection and staging of liver cancer than CT.[16] Therefore, 4-dimensional magnetic resonance imaging (4DMRI) is an ideal way to delineate targets in primary liver cancer, which can capture organ and tumor movement throughout the respiratory cycle.[17,18]

Several MRI-guidance systems have been used in clinical treatment in recent years, and several research groups have made substantial progress towards the integration of 4DMRI in the clinical workflow.[19-21] van de Lindt et al[22] validated the implementation for 4DMRI guided liver stereotactic body radiation therapy workflow in MRI-linac. And Hoffmann et al[23] believe that prototype MR-integrated proton therapy systems will be developed within the next 5 to 10 years. There are many multinational research efforts to incorporate MR imaging into a radiation therapy treatment system.[24] Therefore, it is important to delineate the target of tumor with 4DMRI in future radiotherapy.

With the development of technology and equipment, 4DMRI technology has been increasingly applied. One study by Zhang et al[25] has described the difference in delineation of lung tumor between 4DCT and 4DMRI, they found the average gross tumor volumes (GTVs) are similar between 4DCT and T2w-4DMRI, but smaller in T1w MRI. Another 4DMRI study on the normal tissues shown that the internal organ-at-risk volume (IRV) is 20 to 50% larger than organ at risk (OAR) volumes.[26] However, the appearance of the lesion depends on the difference in signal intensity between the lesion and surrounding normal organs. Therefore, the appearance in 4DMRI of liver tumor may have some differences from lung cancer.[27] To provide a better reference for accurate delineation of liver cancer targets, we compared and discussed the clinical implications of liver tumor delineation using 4DCT and 4DMRI in 23 cases of liver cancer.

Materials and Methods

Patients

Twenty-three patients with hepatic tumors who received radiation therapy between June 2019 and August 2020 were included in this study. The group consisted of 9 patients with tumors in the right posterior segment, 7 in the right anterior segment, 4 in the medial segment of the left lobe of the liver, and 3 in the left lateral lobe of the liver. The patients ranged in age from 33 to 67
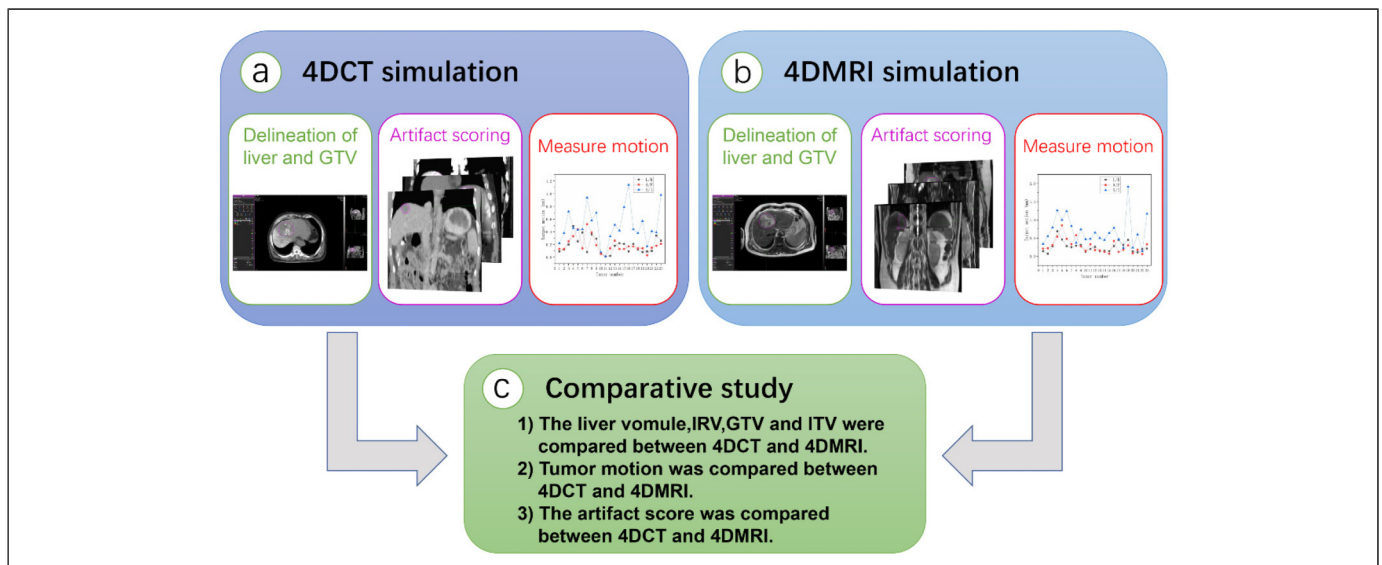
Figure 1. Workflow for the comparison of 4DCT and 4DMRI in this study.
Abbreviations: 4DCT, 4-dimensional computed tomography; 4DMRI, 4-dimensional magnetic resonance imaging.

years old, with a median age of 59 years. This study was approved by the Ethics Review Committee of Shandong Cancer Hospital and Institute (approval No. 201906008). This study is retrospective and the data are anonymous, the requirement for informed consent was therefore waived.

Image Acquisition of 4DCT

All patients underwent 4DCT scan in a free-breathing, uncoached state helical CT scanner (Brilliance Big Bore, Philips Healthcare). The patient was asked to place both arms above the head, and a patient body immobilization mold was prepared in the CT room. The scan range was from 3 to 4 cm above the diaphragm to the lower pole of the right kidney. The voxel size was $0.97\,mm \times 0.97\,mm \times 3\,mm$. A Varian RPM system module fluorescent labeling point device was placed approximately 5 to 10 cm inferior to the xiphoid process of the sternum as the respiratory surrogate for

retrospective amplitude-binned 4DCT reconstruction. The 4DCT data were sorted into 10 respiratory phase bins and named $Phase_0$, $Phase_{10}$ … $Phase_{90}$, wherein $Phase_0$ is the end expiratory phase, $Phase_{50}$ is the end inspiratory phase, and the rest are intermediate phases (Figure 1A).

Image Acquisition of 4DMRI

All patients underwent 4DMRI in the treatment position on the same day, approximately 5 to 6 h after the 4DCT scan. 4DMRI images were obtained on an INGENIA 3.0T scanner (Philips Healthcare) using the navigator-triggered T2w-TSE-4Dbelt sequence with an ACQ voxel size of $1.41\,mm \times 1.61\,mm \times 5\,mm$, REC voxel size of $0.94\,mm \times 0.94\,mm \times 5\,mm$, $TR = 772\,ms$, $TE = 100\,ms$, slice thickness of 5 mm. The navigator was set on the right diaphragm dome, all 4DMRI scans took a similar time of approximately 5 min. Upon the start of the 4DMR measurement the breathing cycle is measured to
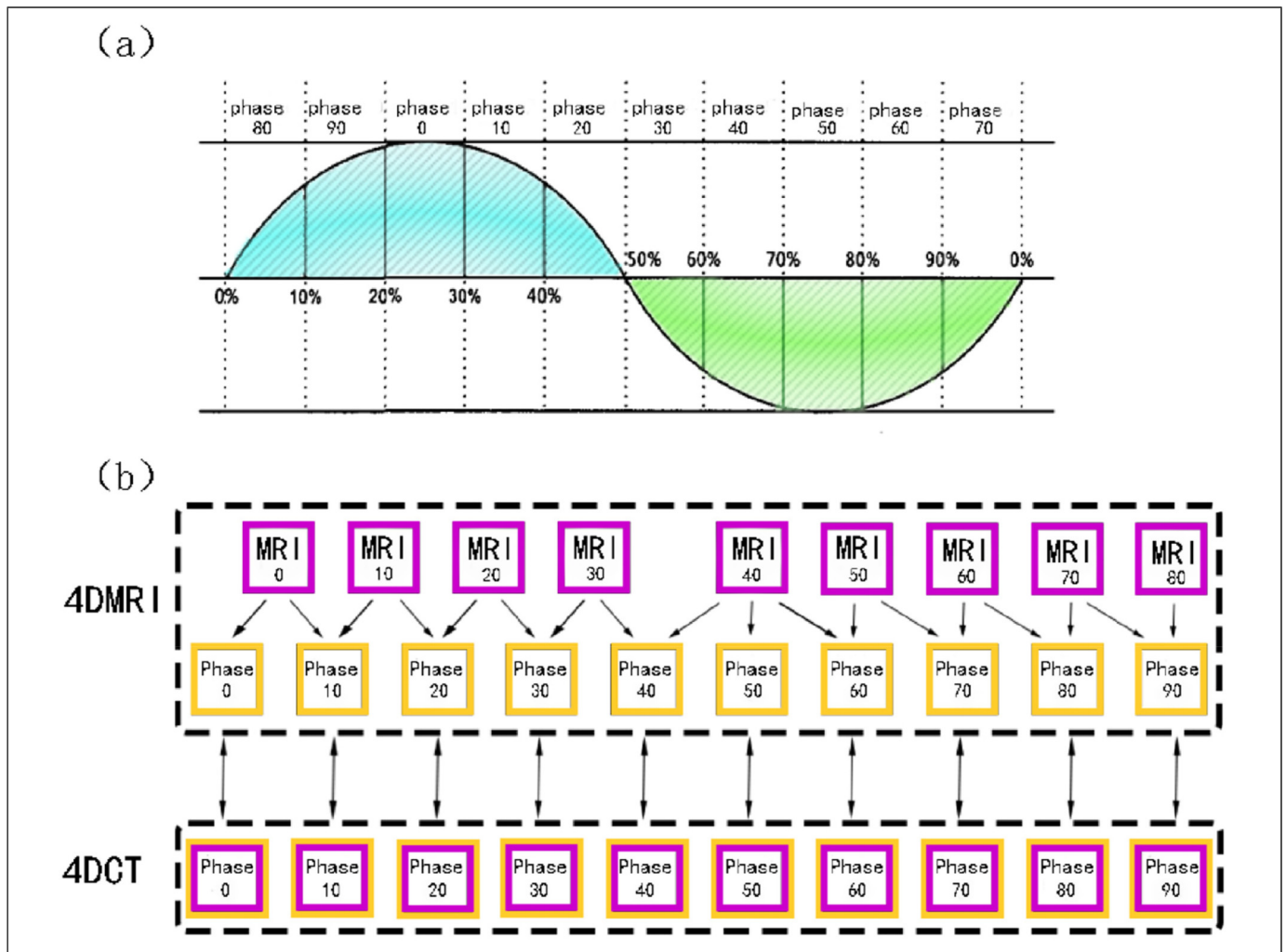
Figure 2. (A) A sample graph of respiratory curve for patients (0%-90% means that the breath curve is divided into 10 parts, the blue area is the inspiratory phase, and the green area is the expiratory phase). (B) The respiratory phase of T2w-4DMRI and 4DCT (The purple box is the acquired phase bins in 4DCT and 4DMRI and yellow box is the phase bins used for comparison).
Abbreviations: 4DCT, 4-dimensional computed tomography; 4DMRI, 4-dimensional magnetic resonance imaging.
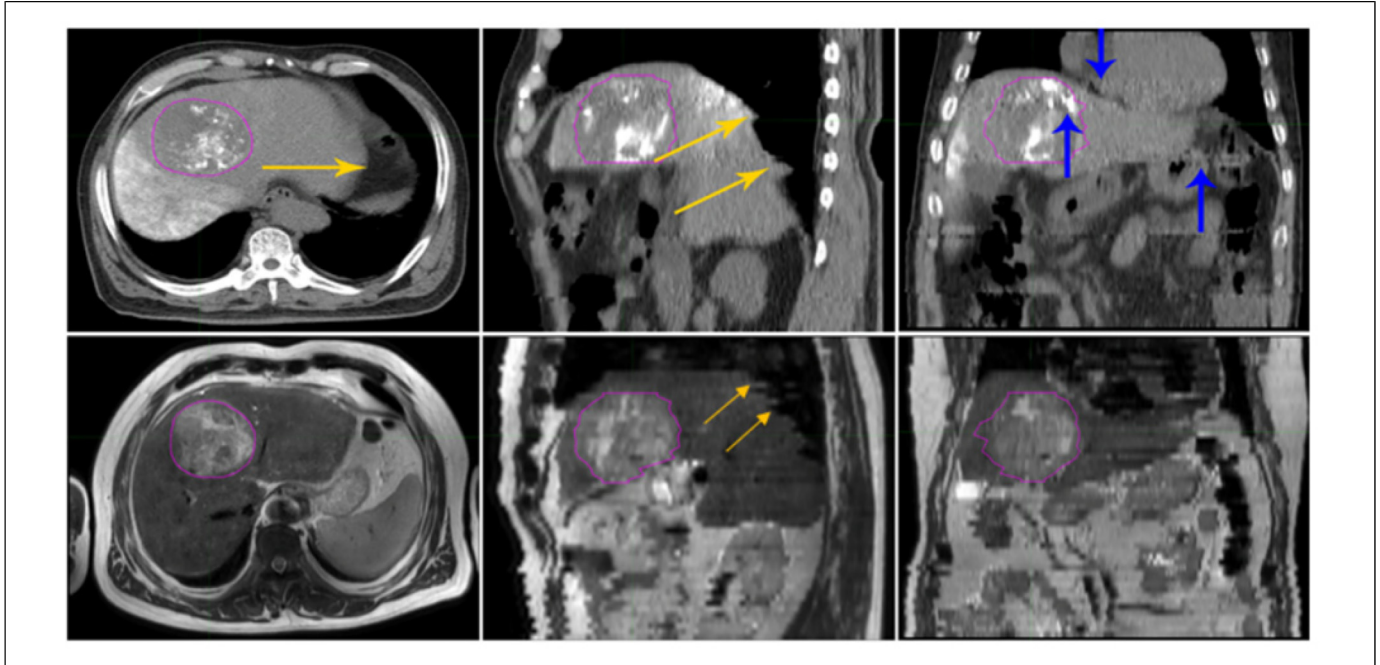
Figure 3. Schematic illustration of respiratory image artifacts in 4DCT and 4DMRI. (Double structure artifact was marked with a orange arrow, and interpolation artifact was marked with a blue arrow).
Abbreviations: 4DCT, 4-dimensional computed tomography; 4DMRI, 4-dimensional magnetic resonance imaging.

determine the inhale-exhale distance, from this the different bins are defined that are filled during continuous scanning, which were sorted into 8 respiratory phase bins and named MRI_0, MRI_{10} … MRI_{70}, wherein MRI_0 is the end phase of expiratory therapy, MRI_{40} is the end phase of inspiratory therapy, and the rest are intermediate phases (Figure 1B).

GTV Contouring and ITV Definition

One radiologist and one radiation oncologist jointly delineated the liver tumor based on the patient's previous imaging data and iodide deposition and tumor changes. The IRV and internal target volume (ITV) were automatically generated by

MIMv6.5.6 software integrating the livers and GTVs of all phases, respectively. The same sketcher completed all GTVs and livers to avoid differences in organ delineations between different sketchers.

Comparison of Multiple Datasets in 4DCT and 4DMRI

All tumors were classified into 3 classes: small tumor (Tumor 1-7) was less than 10 cm^3, medium tumor (Tumor 8-16) was 10 to 100 cm^3, and large tumor (Tumor 17-23) was more than 100 cm^3. Then, we compared the following aspects (Figure 1C):

Table 1. Summary of the Results in Average Volume, GTV Motion, and Artifact Scoring in 4DCT and 4DMRI.

	4DCT	4DMRI
Average volume ($\bar{x} \pm s$, cm^3)		
Liver	1483.84 ± 473.88	1543.19 ± 495.77
IRV	1674.22 ± 494.25	1785.22 ± 513.38
GTV	161.46 ± 280.29	136.42 ± 231.27
ITV	188.56 ± 307.57	166.12 ± 270.43
GTV centroid motion (median/mean/range, mm)		
L/R	1.8/1.9/ (0.1-4.9)	2.5/2.6/ (0.7-6.9)
A/P	1.5/1.9/ (0.1-5.2)	2.6/2.8/ (0.6-8.5)
S/I	4.4/5.0/ (0.1-11.4)	6.0/6.9/ (1.4-19.1)
Artifact scoring		
C1	52.2% (12/23)	82.6% (19/23)
C2	47.8% (11/23)	17.4% (4/23)

Abbreviations: 4DCT, 4-dimensional computed tomography; 4DMRI, 4-dimensional magnetic resonance imaging; IRV, internal organs at risk volume; GTV, gross tumor volume; ITV, internal target volume.

Table 2. The Difference of GTV Between 4DCT and 4DMRI (cm^3).

Tumor	4DCT		4DMRI		Difference	
	Mean	St dev	Mean	St dev	4DMRI-4DCT	Percentage (%)
1	0.45	0.15	1.52	0.66	1.07	235.5
2	1.07	0.26	1.86	0.55	0.79	73.3
3	2.64	0.71	1.62	0.64	−1.03	−38.8
4	3.26	0.64	2.70	0.85	−0.56	−17.2
5	5.99	0.57	3.84	0.39	−2.15	−35.9
6	7.08	1.48	4.17	0.40	−2.92	−41.2
7	7.75	1.10	6.32	0.79	−1.44	−18.5
8	10.81	0.05	14.51	1.20	3.70	34.3
9	12.02	1.09	13.28	1.36	1.26	10.5
10	13.33	0.46	6.92	1.21	−6.41	−48.1
11	20.92	1.20	10.07	1.28	−10.85	−51.9
12	21.07	0.08	11.62	1.04	−9.45	−44.8
13	27.89	2.76	9.66	2.32	−18.22	−65.3
14	32.47	2.30	20.02	1.44	−12.45	−38.3
15	41.61	4.24	12.77	1.04	−28.84	−69.3
16	48.10	4.29	26.01	5.11	−22.09	−45.9
17	205.89	15.57	186.41	7.68	−19.48	−9.5
18	298.89	4.73	241.53	8.53	−57.35	−19.2
19	323.89	8.23	338.92	9.10	15.03	4.6
20	369.50	9.62	313.79	5.87	−55.71	−15.1
21	431.18	20.70	422.22	10.08	−8.96	−2.1
22	700.52	6.71	669.38	5.71	−31.15	−4.5
23	1127.31	6.76	818.48	11.85	−308.83	−27.4
Average	161.46	4.07	136.42	3.44	−25.04	−15.5

Abbreviations: 4DCT, 4-dimensional computed tomography; 4DMRI, 4-dimensional magnetic resonance imaging; GTV, gross tumor volume.

(1) Comparison of liver volume, IRV, GTV, and ITV in 4DCT and 4DMRI.

To better compare the 10 respiratory phase bins of 4DCT, we divided the 8 breath phases of MRI into 10 respiratory phase bins by interpolation that performed between the volumes of adjacent respiratory phases, as shown in Figure 2.

(2) Comparison of motion range in 4DCT and 4DMRI.

The GTV centroid motion between end-inspiration and end-expiration is compared in 4DCT and 4DMRI. In addition, the motions of the GTV in 6 directions (left, right, anterior, posterior, superior, and inferior) determined by 4DCT and 4DMRI based on tumor edge differences were compared.

(3) Artifact scoring

We divide artifacts into no or moderate artifacts (C1) and severe artifacts (C2) based on the research methods of others.[15] C1 are maximum 4 double structure artifacts and no interpolation artifacts, otherwise are C2.

Double structure artifacts are caused by respiratory motion irregularity during image acquisition, as shown in Figure 3. Interpolation artifacts indicate a lack of sufficient projection data to reconstruct transversal images at the corresponding couch position and breathing phase. Therefore, interpolation artifacts in the central image area directly leads to an artifact score of C2.[15,28]

Statistical Evaluation

Statistical analysis was performed using SPSS 24.0 software (IBM CORP.) using descriptive statistics and bar chart to display all motion data. The Wilcoxon signed-rank test was used to investigate the relationship between 4DCT and 4DMRI. The factors tested were liver volume, GTV, ITV, and tumor motion. $P < .05$ was considered statistically significant.

Results

The Difference of Liver Volume, IRV, GTV, and ITV between 4DCT and 4DMRI

Table 1 is the summary of the results, whereas Table 2 shows the difference percentage of GTV from all 23 tumors. The liver volume and IRV determined by 4DMRI were larger than 4DCT, the average value of differences was 59.35 cm^3 (4.0%) and 111.00 cm^3 (6.6%), respectively. Conversely, the GTV and ITV in 4DMRI were less than 4DCT, the average value of differences was, respectively, 25.04 cm^3 (15.5%) and 22.44 cm^3 (11.9%), with statistical significance ($P = .002$, $P = .006$, two-sided Wilcoxon rank-sum test). In 78.3% of cases show smaller mean GTV in 4DMRI than 4DCT, as shown in Figure 4.
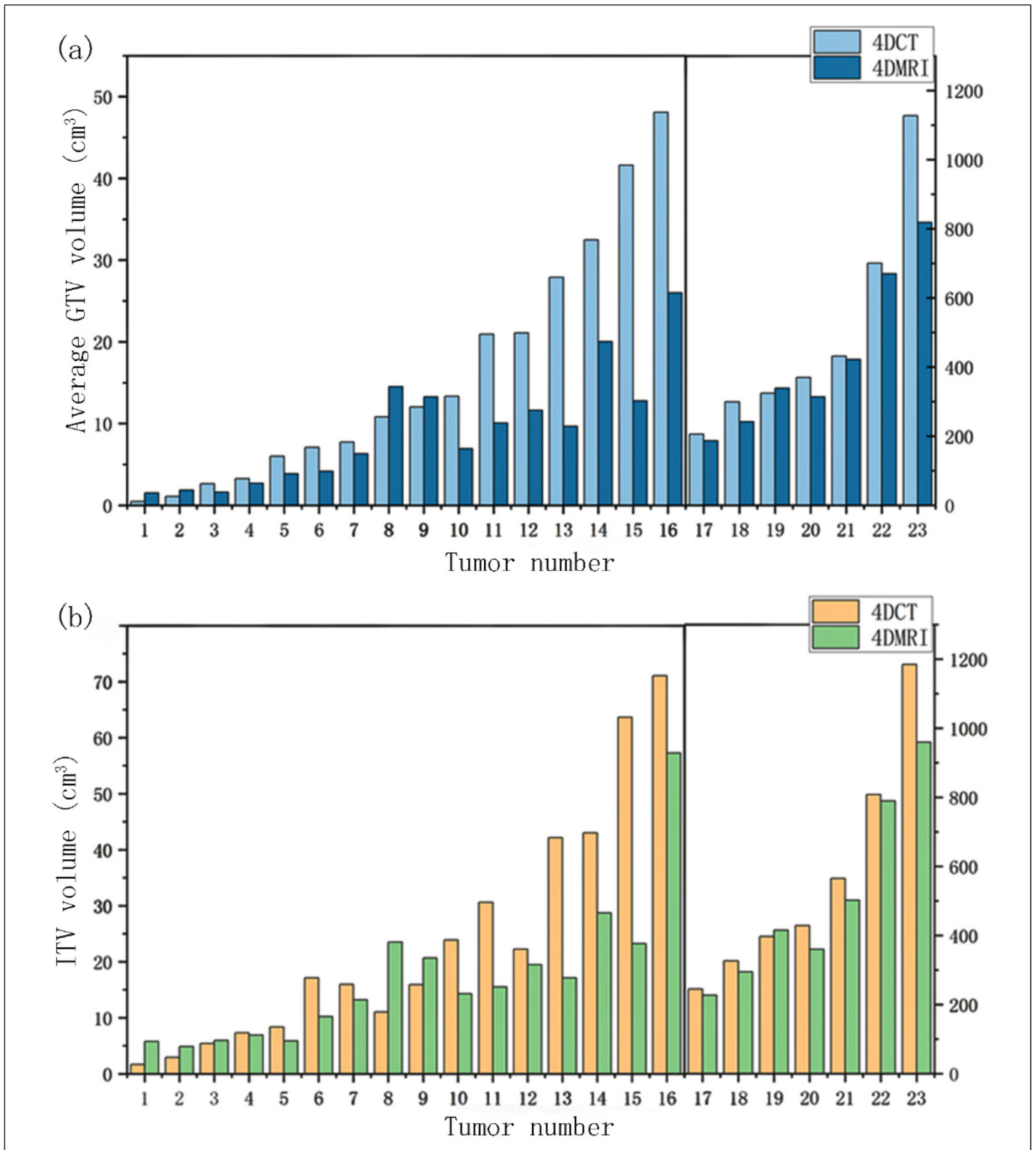
Figure 4. A plot of all delineated the average GTV and ITV in 4DCT and 4DMRI (The left coordinate axis was used for 1 through 16 tumors, and the right coordinate axis was used for 17 through 23 tumors).
Abbreviations: GTV, gross tumor volume; ITV, internal target volume; 4DCT, 4-dimensional computed tomography; 4DMRI, 4-dimensional magnetic resonance imaging.

The variation in GTV within the breathing cycle of 4DMRI (1.5%) is smaller than 4DCT (3.8%), as shown in Table 3, which indicates the better delineation reproducibility in the 4DMRI with respect to the 4DCT. The average GTV ratios (GTV^{4DMRI}/GTV^{4DCT}) of $Phase_0$ and $Phase_{50}$ were 0.86 and 0.83, respectively.

Table 3. Variation of GTV Within the Breathing Cycle of 4DCT and 4DMRI ($\bar{x} \pm s$, cm^3).

Phase	4DCT	4DMRI	P-value
Phase$_0$	158.63 ± 281.75	135.72 ± 232.36	.013
Phase$_{10}$	158.61 ± 281.11	136.06 ± 232.27	.020
Phase$_{20}$	159.28 ± 278.85	136.58 ± 231.42	.006
Phase$_{30}$	160.45 ± 279.83	137.16 ± 231.84	.010
Phase$_{40}$	163.69 ± 281.42	137.90 ± 233.19	.001
Phase$_{50}$	164.32 ± 280.36	136.94 ± 232.46	.001
Phase$_{60}$	163.14 ± 280.87	136.67 ± 231.14	.002
Phase$_{70}$	160.88 ± 280.05	135.65 ± 229.21	.003
Phase$_{80}$	161.32 ± 280.36	135.09 ± 229.49	.002
Phase$_{90}$	158.05 ± 279.52	135.36 ± 231.29	.012

Abbreviations: 4DCT, 4-dimensional computed tomography; 4DMRI, 4-dimensional magnetic resonance imaging; GTV, gross tumor volume.

Variation in GTV Motion between 4DCT and 4DMRI

The mean value, median value, and motion range of GTV centroid estimation in the L/R, A/P, and S/I directions of 4DCT and 4DMRI are shown in Table 1, and the corresponding mean value of GTV motion is shown in Figure 5. In 69.6% of cases, GTV centroid motion was similar to or greater in 4DMRI than in 4DCT. In the L/R, A/P, and S/I directions, the mean differences in GTV centroid motion between 4DCT and T2w-4DMRI were 0.7, 0.9, and 1.9 mm, respectively. The difference between 4DCT S/I motion estimates and the motion estimates derived from 4DMRI motion data was statistically significant ($P = .048$, two-sided Wilcoxon rank-sum test).

The motion of GTV edges as the maximum among all slices was also evaluated in 6 directions (left, right, anterior, posterior, superior, and inferior), and the corresponding data statistics are shown in Table 4. 4DMRI motion was larger than 4DCT motion for the left, right, anterior, posterior, superior, and inferior direction in 60.9%, 69.6%, 52.2%, 60.9%, 52.2%, and 60.9% of patients, respectively.

Differences in Artifact Classes in 4DCT and 4DMRI

The artifact class frequencies assigned to the 23 lesions in the 4DCT data were 52.2% (12/23) for moderate artifacts and 47.8% (11/23) for severe artifacts, whereas the frequencies in the 4DMRI data were 82.6% (19/23) and 17.4% (4/23) for moderate artifacts and severe artifacts, respectively.

Discussion

4DMRI is a useful technique for tumor delineation and assessment of motion due to its excellent soft-tissue contrast with zero radiation hazard. We demonstrated the feasibility of using 4DMRI to delineate GTV and ITV for liver cancer radiotherapy by comparing 4DMRI with 4DCT. We quantified the differences between 4DCT and 4DMRI in the target morphology and motion of liver cancer. Our data showed that, compared with 4DCT, 4DMRI might help reduce the uncertainty of
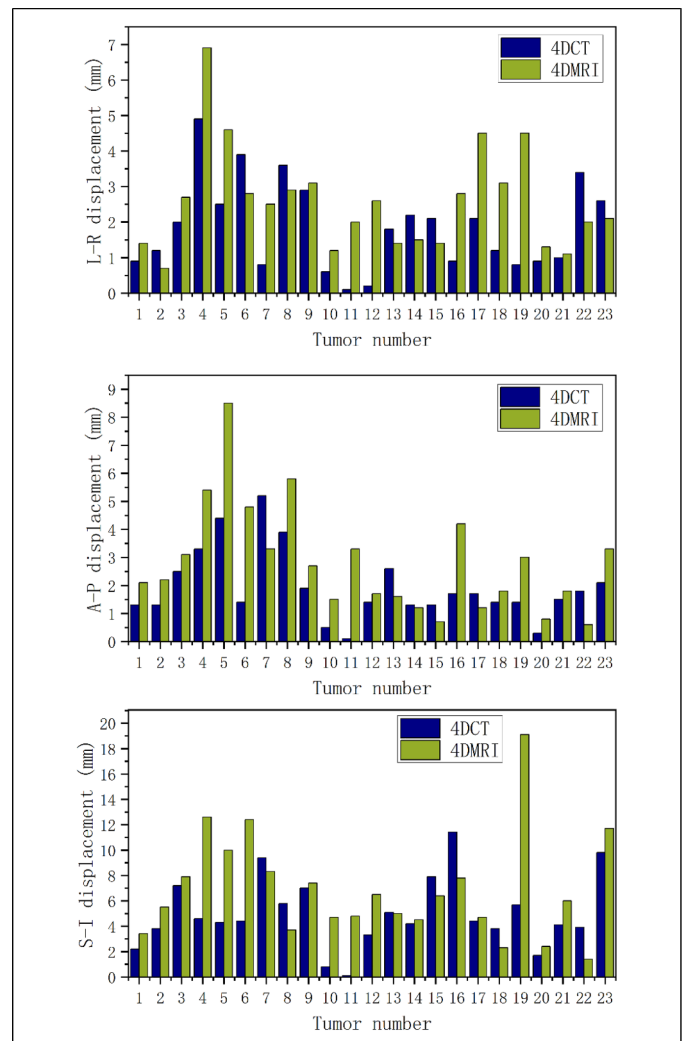
Figure 5. The mean of absolute values of GTV displacement among all phases in the left-right (above), anterior-posterior (mid), and superior-inferior (below) direction of 4DCT and T2w-4DMRI. Abbreviations: GTV, gross tumor volume; 4DCT, 4-dimensional computed tomography; 4DMRI, 4-dimensional magnetic resonance imaging.

delineating liver tumors by providing images with excellent soft-tissue contrast and fewer artifacts. In addition, 4DMRI can detect differences in hepatic intrafraction tumor motion better than 4DCT, which may have clinical significance.

In this study, there were significant differences in liver volume and GTV between 4DCT and 4DMRI. The average GTV and ITV decreased by 15.5% and 11.9% when changing from 4DCT to 4DMRI, respectively. The tumor variation between 4DCT and 4DMRI in this study is comparable to the difference in CT and specimen reported by Lampen-Sachar et al, which showed that the GTV from CT is 18.3% greater than that from pathological specimens.[29] This indicates that 4DMRI can significantly improve the delineation accuracy of liver cancer targets. It is worth mentioning that Tumor 1, 2, 11, 13, and 15 (5 of 23 cases: 21.7%) show significant difference in volume between 4DCT and 4DMRI, all of which

Table 4. Pairwise Differences of GTV Edges Motion Between 4DCT and 4DMRI in the Left, Right, Anterior, Posterior, Superior, and Inferior Directions.

Parameter	Left	Right	Anterior	Posterior	Superior	Inferior
Patients with larger 4DMRI motion compared with 4DCT	14 (60.9%)	16 (69.6%)	12 (52.2%)	14 (60.9%)	12 (52.2%)	14 (60.9%)
Differences between 4DCT and 4DMRI (mm)	3.6 (0.6-8.8)	2.7 (0.2-6.6)	1.7 (0.2-6.4)	2.9 (0.1-9.2)	3.9 (0.3-11)	4.5 (0.5-14.2)
Patients with larger 4DMRI motion compared with 4DCT that is clinically significant (>3 mm)	8 (34.8%)	5 (21.7%)	1 (4.3%)	5 (21.7%)	6 (26.1%)	7 (30.4%)
Patients with smaller 4DMRI motion compared with 4DCT	9 (39.1%)	7 (30.4%)	11 (47.8%)	8 (34.8%)	11 (47.8%)	9 (39.1%)
Differences between 4DCT and 4DMRI (mm)	2.4 (0.1-8.5)	1.8 (0.3-4.7)	4.7 (0.3-8.8)	3.3 (0.1-8.3)	3.3 (0.4-7.2)	4.3 (1.4-9.5)
Patients with smaller 4DMRI motion compared with 4DCT that is clinically significant (>3 mm)	3 (13.0%)	2 (8.7%)	5 (21.7%)	3 (13.0%)	6 (26.1%)	6 (26.1%)

Values are number (percentage) or median (range).

Abbreviations: 4DCT, 4-dimensional computed tomography; 4DMRI, 4-dimensional magnetic resonance imaging; GTV, gross tumor volume.

belong to small or medium tumor. The tumor variation between imaging modalities in this study is consistent with previous finding by Zhang et al,[25] despite differences in tumor type. Zhang et al[25] based on 16 lung cancer patients, illustrated that the average GTV in 4DMRI was smaller than that in 4DCT, and the small tumor that are less than 100 cm[3] also showed significant discrepancies. Furthermore, the prescription dose has to cover the planning tumor volume (PTV) in radiation therapy. PTV consists of ITV plus a margin that may include nearby OARs, which is crucial to determine the dose-limiting toxicity.[30] The greater certainty of target and normal tissue localizations promises to decrease the normal tissue complication probability (NTCP) by sparing additional normal tissue adjacent to the moving target.[18] We found that the liver volume and IRV increased by 4.0% and 6.6%, respectively, from 4DCT to 4DMRI, which may have significance for tumor control probability (TCP) and for reducing the probability of NTCP.

In this study, the range of GTV centroid motion was 6.9, 8.5, and 19.1 mm in the S/I, A/P, and L/R directions, comparable to liver tumor motion reported using cine-MRI by Kirilova et al[31] We found that the mean differences between the 4DCT and 4DMRI measures of the GTV centroid were 0.7, 0.9, and 1.9 mm in the S/I, A/P, and L/R directions, respectively. Interestingly, in other studies, 4DCT was compared with fluoroscopy, film MRI, and 4DCBCT, and all found that 4DCT underpredicted tumor motion.[12,32,33] In addition, this also explains why the variation in ITV in 4DMRI and 4DCT was smaller than that with the GTV. The ITV expands the boundary of the target for organ movement and integrates the GTV throughout the respiratory cycle. Although the GTV in 4DMRI is smaller than that in 4DCT, the motion range is larger, elongating the ITV and results in a smaller ITV difference between 4DCT and 4DMRI.

Artifacts were reported to affect delineation of the GTV.[34] In the present study, the number of severe artifacts decreased from 47.8% to 17.4% in 4DMRI compared with 4DCT, corresponding to a significantly improved image quality and guaranteed accurate delineation of the target of primary liver cancer. Double structure artifacts are caused by respiratory motion

irregularity during image acquisition, while interpolation artifacts are due to lack of sufficient projection data for reconstruction of images at the corresponding couch position and breathing phase.[15,28] Recent data show that most 4DCT images are still affected by artifacts.[35] Li et al compared the 4DMRI image quality between external and internal surrogating signal for reconstruction of 4DMRI images in 2017, they stated that navigator-triggered 4DMRI image quality is far superior.[36] Moreover, the navigator-triggered 4DMRI is less prone to motion artifacts caused by irregular breathing, as it is using an internal surrogate.[37] Therefore, there are less artifacts in 4DMRI due to the different reconstruction methods compared with 4DCT. Significantly, 4DMRI carries a unique artifact similar to binning artifacts but only in the heart and major arteries/veins. Therefore, the artifact does not affect the delineation of the liver target.[25,38] To our knowledge, this is the first study that combines artifact scoring and assessment of target motion to compare the evaluation of 4DCT and 4DMRI to determine the target of primary liver cancer. However, the artifact scoring in this study is relatively simple, and follow-up studies can develop more detailed scoring standards for image rank, which may have reference significance for future clinical image quality assessment and target delineation.

Mahmoud et al[39] showed that T2-weighted images were superior to other weighted images in detecting liver cancer. Therefore, T2w-4DMRI is a promising technique for clinical liver tumor delineation and was used in our study. Although the larger slice thickness in 4DMRI (5 mm) for 4DCT (3 mm), 4DMRI detects larger liver volume and GTV motion compared with 4DCT, which proved that the difference of slice thickness no significant affect our results. Several algorithms exist for 4DMRI reconstruction, but the results of this study are only valid for T2-weighted and navigator-triggered 4DMRI and cannot be extended to all algorithms.

This study quantified the comparison between 4DCT and 4DMRI in delineating targets in primary liver cancer, whereas the dose advantage of 4DMRI in delineating targets has not been evaluated. The synthetic CT generation methodologies used in MRI-only radiotherapy was systematically

evaluated by Johnstone et al[40] and shown high accuracy. In addition, van de Lindt et al[41] evaluated the deformable CT-MRI registration steps based on the 4DMRI technique. However, miss-registration will produce segmentation errors between CT and MR.[24] Therefore, based on the current study, dose calculations by reflecting the 4DMRI contours on the 4DCT will be added in future studies, which will provide more important clinical guidance for target delineation in radiotherapy.

Conclusions

This study demonstrated the feasibility of using 4DMRI to delineate the target of primary liver cancer in radiotherapy. Compared with 4DCT, T2-weighted and navigator-triggered 4DMRI has fewer artifacts and more accurate motion assessment, which will help reduce the uncertainty in delineating the target of liver cancer.

Declaration of Conflicting Interests

The authors declared no potential conflicts of interest with respect to the research, authorship, and/or publication of this article.

Funding

Ethical Approval

All procedures performed in studies involving human participants were in accordance with the ethical standards of the institutional and/or national research committee and with the 1964 Helsinki declaration and its later amendments or comparable ethical standards. For this type of study formal consent is not required.

ORCID iD

Yukai Chen https://orcid.org/0000-0002-9762-3022

References

1. Bray F, Ferlay J, Soerjomataram I, Siegel RL, Torre LA, Jemal A. Global cancer statistics 2018: GLOBOCAN estimates of incidence and mortality worldwide for 36 cancers in 185 countries. *CA Cancer J Clin*. 2018;68(6):394-424. doi:10.3322/caac.21492

2. Xu G, Zhu L, Wang Y, Shi Y, Gong A, Wu C. Stattic enhances radiosensitivity and reduces radio-induced migration and invasion in HCC cell lines through an apoptosis pathway. *Biomed Res Int*. 2017;2017:1–9. doi:10.1155/2017/1832494

3. Choi C, Koom WS, Kim TH, et al. A prospective phase 2 multicenter study for the efficacy of radiation therapy following incomplete transarterial chemoembolization in unresectable hepatocellular carcinoma. *Int J Radiat Oncol Biol Phys*. 2014; 90(5):1051-1060. doi:10.1016/j.ijrobp.2014.08.011

4. Que J, Kuo H-T, Lin L-C, et al. Clinical outcomes and prognostic factors of cyberknife stereotactic body radiation therapy for unresectable hepatocellular carcinoma. *BMC Cancer*. 2016;16(1):451. doi:10.1186/s12885-016-2512-x

5. Keane FK, Wo JY, Zhu AX, Hong TS. Liver-directed radiotherapy for hepatocellular carcinoma. *Liver Cancer*. 2016;5(3):198-209. doi:10.1159/000367764

6. Velec M, Moseley JL, Eccles CL, et al. Effect of breathing motion on radiotherapy dose accumulation in the abdomen using deformable registration. *Int J Radiat Oncol Biol Phys*. 2011; 80(1):265-272. doi:10.1016/j.ijrobp.2010.05.023

7. Rosu M, Dawson LA, Balter JM, McShan DL, Lawrence TS, Ten Haken RK. Alterations in normal liver doses due to organ motion. *Int J Radiat Oncol* Biol* Phys*. 2003;57(5):1472-1479. doi: 10.1016/j.ijrobp.2003.08.025

8. Lock MI, Klein J, Chung HT, et al. Strategies to tackle the challenges of external beam radiotherapy for liver tumors. *World J Hepatol*. 2017;9(14):645–656. doi: 10.4254/wjh.v9.i14.645

9. Akino Y, Oh R-J, Masai N, Shiomi H, Inoue T. Evaluation of potential internal target volume of liver tumors using cine-MRI. *Med Phys*. 2014;41(11):111704. 10.1118/1.4896821

10. Keall PJ, Mageras GS, Balter JM, et al. The management of respiratory motion in radiation oncology report of AAPM task group 76. *Med Phys*. 2006;33(10):3874-3900. doi:10.1118/1.2349696

11. Iramina H, Nakamura M, Iizuka Y, et al. The accuracy of extracted target motion trajectories in four-dimensional cone-beam computed tomography for lung cancer patients. *Radiother Oncol*. 2016;121(1):46-51. doi:10.1016/j.radonc.2016.07.022

12. Ge J, Santanam L, Noel C, Parikh PJ. Planning 4-dimensional computed tomography (4DCT) cannot adequately represent daily intrafractional motion of abdominal tumors. *Int J Radiat Oncol Biol Phys*. 2013;85(4):999-1005. doi:10.1016/j.ijrobp.2012.09.014

13. Purdie TG, Moseley DJ, Bissonnette JP, et al. Respiration correlated cone-beam computed tomography and 4DCT for evaluating target motion in stereotactic lung radiation therapy. *Acta Oncol*. 2006;45(7):915-922. doi:10.1080/02841860600907345

14. Yamamoto T, Langner U, Loo BWJr., Shen J, Keall PJ. Retrospective analysis of artifacts in four-dimensional CT images of 50 abdominal and thoracic radiotherapy patients. *Int J Radiat Oncol Biol Phys*. 2008;72(4):1250-1258. doi:10.1016/j.ijrobp.2008.06.1937

15. Sentker T, Schmidt V, Ozga AK, et al. 4D CT image artifacts affect local control in SBRT of lung and liver metastases. *Radiother Oncol*. 2020;148:229-234. doi:10.1016/j.radonc.2020.04.006

16. Kierans AS, Elazzazi M, Braga L, et al. Thermoablative treatments for malignant liver lesions: 10-year experience of MRI appearances of treatment response. *AJR Am J Roentgenol*. 2010; 194(2):523-529. doi:10.2214/AJR.09.2621

17. Siebenthal Mv, Székely G, Gamper U, Boesiger P, Lomax A, Cattin P. 4D MR imaging of respiratory organ motion and its

variability. *Phys Med Biol*. 2007;52(6):1547-1564. doi:10.1088/0031-9155/52/6/001

18. Li G, Citrin D, Camphausen K, et al. Advances in 4D medical imaging and 4D radiation therapy. *Technol Cancer Res Treat*. 2008;7(1):67-81.

19. Li G, Liu Y, Nie X. Respiratory-correlated (RC) vs. time-resolved (TR) four-dimensional magnetic resonance imaging (4DMRI) for radiotherapy of thoracic and abdominal cancer. *Front Oncol*. 2019;9:1024. doi:10.3389/fonc.2019.01024

20. Burigo LN, Oborn BM. MRI-guided proton therapy planning: accounting for an inline MRI fringe field. *Phys Med Biol*. 2019;64-(21):215015. doi:10.1088/1361-6560/ab436a

21. Kai D, Patrick N, Christian D, et al. 4D Dose calculation for PBS proton therapy of pancreatic cancer using repeated 4DMRI dataset. *Phys Med Biol*. 2018;63(16):165005. doi: 10.1088/1361-6560/aad43f

22. van de Lindt TN, Fast MF, van den Wollenberg W, et al. Validation of a 4D-MRI guided liver stereotactic body radiation therapy strategy for implementation on the MR-linac. *Phys Med Biol*. 2021;66(10):105010. doi:10.1088/1361-6560/abfada

23. Hoffmann A, Oborn B, Moteabbed M, et al. MR-guided proton therapy: a review and a preview. *Radiat Oncol*. 2020;15(1):129. doi:10.1186/s13014-020-01571-x

24. Das IJ, McGee KP, Tyagi N, Wang H. Role and future of MRI in radiation oncology. *Br J Radiol*. 2019;92(1094):20180505. doi:10.1259/bjr.20180505

25. Zhang J, Srivastava S, Wang C, et al. Clinical evaluation of 4D MRI in the delineation of gross and internal tumor volumes in comparison with 4DCT. *J Appl Clin Med Phys*. 2019;20(9):51-60. doi:10.1002/acm2.12699

26. Zhang J, Markova S, Garcia A, et al. Evaluation of automatic contour propagation in T2-weighted 4DMRI for normal-tissue motion assessment using internal organ-at-risk volume (IRV). *J Appl Clin Med Phys*. 2018;19(5):598-608. doi:10.1002/acm2.12431

27. Altun E, El-Azzazi M, Semelka RC. *Liver Imaging: MRI with CT Correlation*. Oxford, Wiley-Blackwell; 2015.

28. Werner R, Sentker T, Madesta F, Gauer T, Hofmann C. Intelligent 4D CT sequence scanning (i4DCT): concept and performance evaluation. *Med Phys*. 2019;46(8):3462-3474. doi:10.1002/mp.13632

29. Lampen-Sachar K, Zhao B, Zheng J, et al. Correlation between tumor measurement on computed tomography and resected specimen size in lung adenocarcinomas. *Lung Cancer*. 2012;75(3):332-335. doi:10.1016/j.lungcan.2011.08.001

30. Murrell DH, Laba JM, Erickson A, Millman B, Palma DA, Louie AV. Stereotactic ablative radiotherapy for ultra-central lung tumors: prioritize target coverage or organs at risk? *Radiat Oncol*. 2018;13(1):57. doi:10.1186/s13014-018-1001-6

31. Kirilova A, Lockwood G, Choi P, et al. Three-dimensional motion of liver tumors using cine-magnetic resonance imaging. *Int J Radiat Oncol Biol Phys*. 2008;71(4):1189-1195. doi:10.1016/j.ijrobp.2007.11.026

32. Fernandes AT, Apisarnthanarax S, Yin L, et al. Comparative assessment of liver tumor motion using cine-magnetic resonance imaging versus 4-dimensional computed tomography. *Int J Radiat Oncol Biol Phys*. 2015;91(5):1034-1040. doi:10.1016/j.ijrobp.2014.12.048

33. Steiner E, Shieh CC, Caillet V, et al. Both four-dimensional computed tomography and four-dimensional cone beam computed tomography under-predict lung target motion during radiotherapy. *Radiother Oncol*. 2019;135:65-73. doi:10.1016/j.radonc.2019.02.019

34. Persson GF, Nygaard DE, Brink C, et al. Deviations in delineated GTV caused by artefacts in 4DCT. *Radiother Oncol*. 2010;96(1):61-66. doi:10.1016/j.radonc.2010.04.019

35. Werner R, Hofmann C, Mücke E, Gauer T. Reduction of breathing irregularity-related motion artifacts in low-pitch spiral 4D CT by optimized projection binning. *Radiat Oncol*. 2017;12(1):100. doi:10.1186/s13014-017-0835-7

36. Li G, Wei J, Olek D, et al. Direct comparison of respiration-correlated four-dimensional magnetic resonance imaging reconstructed using concurrent internal navigator and external bellows. *Int J Radiat Oncol Biol Phys*. 2017;97(3):596-605. doi:10.1016/j.ijrobp.2016.11.004

37. Paganelli C, Kipritidis J, Lee D, Baroni G, Keall P, Riboldi M. Image-based retrospective 4D MRI in external beam radiotherapy: a comparative study with a digital phantom. *Med Phys*. 2018;45(7):3161-3172. doi:10.1002/mp.12965

38. Brandner ED, Chetty IJ, Giaddui TG, Xiao Y, Huq MS. Motion management strategies and technical issues associated with stereotactic body radiotherapy of thoracic and upper abdominal tumors: a review from NRG oncology. *Med Phys*. 2017;44(6):2595-2612. doi:10.1002/mp.12227

39. Mahmoud BEMH, Elkholy SF, Nabeel MM, et al. Role of MRI in the assessment of treatment response after radiofrequency and microwave ablation therapy for hepatocellular carcinoma. *Egypt J Radiol Nucl Med*. 2016;47(2):377-385. doi:10.1016/j.ejrnm.2016.01.007

40. Johnstone E, Wyatt JJ, Henry AM, et al. Systematic review of synthetic computed tomography generation methodologies for use in magnetic resonance imaging-only radiation therapy. *Int J Radiat Oncol Biol Phys*. 2018;100(1):199-217. doi:10.1016/j.ijrobp.2017.08.043

41. van de Lindt TN, Fast MF, van Kranen SR, et al. MRI-guided mid-position liver radiotherapy: validation of image processing and registration steps. *Radiother Oncol*. 2019;138:132-140. doi:10.1016/j.radonc.2019.06.007